*Thin Solid Films*, *238* (1994) 172–183

# The effect of substrate surface temperature on the morphology and quality of diamond films produced by the oxyacetylene combustion method

K. Bang, A. J. Ghajar and R. Komanduri

*School of Mechanical and Aerospace Engineering, Oklahoma State University, Stillwater, OK 74078 (USA)*

(Received March 16, 1993; accepted August 27, 1993)

**Abstract**

Diamond films were synthesized using an oxyacetylene flame on a molybdenum substrate mounted on a water-cooled copper block. The morphology and quality of the synthetic diamond films produced depend on several factors including the substrate temperature, gas flow rates and their ratio, and substrate position. The substrate temperature profile was shown to be influenced by the coolant flow rate, nozzle size, substrate position on the heat sink, substrate position in the combustion flame, and the total flow rate of mixed gas (acetylene and oxygen). In this paper, the effects of substrate temperature and nozzle size on the morphology and quality of diamond films are discussed. Fine-gage thermocouples were used to measure the temperature distribution in the substrate during the process. Scanning electron microscopy of the produced diamond films is used to show the variation of crystal morphology.

## 1. Introduction to chemical vapor deposition (CVD) diamond synthesis

Diamond technologically is a fascinating material. It has many unique properties including the highest hardness, high wear resistance, low coefficient of friction, high thermal conductivity, high chemical inertness, high electrical resistivity, optical transparency, and high sonic speed, and consequently its synthesis has been for centuries a great scientific challenge.

The unique properties of diamond have enabled its use in a variety of manufacturing applications. Diamond (both natural and synthetic) has long been used to cut, drill, mine, and mill everything from the hardest rock to the softest aluminum. Now synthetic diamond films are rapidly taking on new roles with potential to coat aircraft turbine blades, microprocessor chips, surgical instruments, and light-emitting diodes. Potential new uses for diamond films range from supercomputer heat sinks and heat-seeking missile windows to such mundane things as gourmet knives and scratch-proof sunglasses.

The growing demand for this unique material has fueled efforts to produce diamond synthetically. The modern era of low pressure diamond synthesis under metastable conditions began in the 1980s using activated CVD techniques. However, the CVD process was commercially limited by its low growth rates ($\sim 1\ \mu m\ h^{-1}$). Excellent reviews of the synthesis of diamond under metastable conditions have been presented by DeVries [1] and Angus and Hayman[2].

During the past decade a number of activated CVD methods for low-pressure diamond deposition have been developed with the aim of increasing the growth rate [3]. Among the activated processes for CVD diamond synthesis, the oxyacetylene combustion approach is particularly exciting in view of its simplicity and low cost of equipment. The method, originally developed by Hirose of Japan in 1988, uses an oxyacetylene welding torch with a slightly fuel-rich (acetylene) mixture (see Fig. 1 for a schematic of the apparatus). The oxyacetylene flame sketched in Fig. 1 shows three regions: the inner cone, which bounds the $O_2$–$C_2H_2$ flame front; the $C_2H_2$ feather zone, where excess $C_2H_2$ burns with $O_2$ which diffuses into the flame from the surrounding air (this only appears when the mole ratio of $C_2H_2$ to $O_2$ is greater than unity), and the outside flame, where the CO and $H_2$ produced in the inner cone and acetylene feather zone are burned to produce $CO_2$ and $H_2O$. The flame temperature in the inner cone varies with the ratio $R$ of $O_2$ to $C_2H_2$ gas flow, from 3162 °C for $R = 1.5$ to 2960 °C for $R = 0.8$ [4]. The length of the inner cone depends on the total flow rate and nozzle size, and the length and width of the acetylene feather depend on the flow ratio and total gas flow rate. Diamond growth on the substrate was observed only in the second zone, namely, the acetylene feather. The acetylene feather envelopes the substrate and shields the

0040-6090/94/$7.00

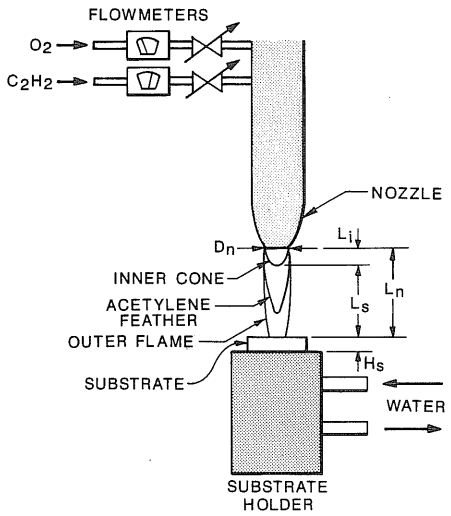


Fig. 1. Schematic of the oxyacetylene experimental set-up.

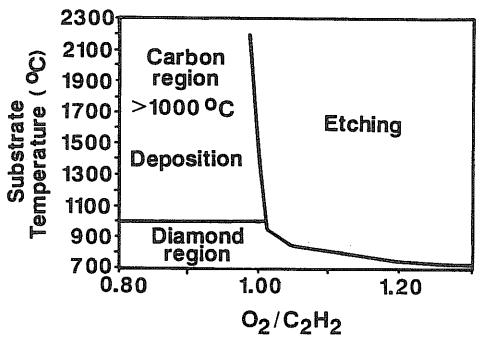


Fig. 2. Maximum temperature for carbon deposition at 1 bar as a function of the flame stoichiometry [6].

diamond film from oxidation. As the flame temperatures are very high ( ~3000 °C), the substrate is cooled by mounting it on a water-cooled copper block in order to provide the appropriate conditions for diamond nucleation and growth. This technique offers a very simple and economical means of synthesizing diamond films. As the diamond growth takes place under atmospheric conditions, expensive vacuum chambers and appropriate equipment are not required. The flame provides its own environment for diamond growth and the quality of the film is largely dependent on substrate temperature profile, gas flow ratio of oxygen to acetylene, and substrate position. The substrate temperature profile, in turn, is influenced by such process variables as coolant flow rate, nozzle size, substrate position on the heat sink, substrate position in the combustion flame, and total flow rate of mixed gas (oxygen and acetylene). The influence of these parameters on the substrate temperature profile and consequently the morphology and quality of diamond films for this interesting new technique is yet to be fully exploited. In a previous paper [5] the influence of these parameters on the substrate temperature profile was characterized. In this paper the effect of the substrate temperature profile, resulting from changing the values of the process variables, on the morphology and quality of diamond films produced by the oxyacetylene method will be studied. In addition, the effect of nozzle size on the quality of the diamond films will be discussed.

## 2. Background

A brief review of the results of some of the important previous investigations on the growth of diamond films (crystal morphology with temperature and gas flow ratio) by the oxyacetylene combustion method will be presented here.

Kosky and McAtee [6] found that formation of solid carbons from gaseous carbons by condensation is dependent on the ratio $R$ of $O_2$ to $C_2H_2$. Figure 2 is a graph of the maximum substrate temperature locus at which solid carbon can form. In fuel-rich flames, *i.e.* $R \leqslant 1.0$, carbon (solid state) will deposit on the substrate from low to high temperatures. The etching–deposition boundary is very steep near $R = 1$ and, for a given flame stoichiometry, relatively small substrate temperature changes will control whether a deposit is produced or an existing deposit is etched. The experimental results of refs. 7–14 showed that the optimal range of $R$ for diamond film deposition was 0.83–1.0.

A characteristic of the diamond film synthesized by CVD methods is that it has a well-defined crystal habit, which depends on the experimental conditions. Matsumoto and Matsui [15] have observed that the morphology of CVD diamond crystals is dominated by cubic and octahedral habits. Figure 3 shows the typical crystal structures of diamond films produced by the oxyacetylene combustion method.

In the high pressure high temperature synthesis of diamond films, a cubic habit is observed at low temperatures. This phenomenon is observed in some CVD methods such as the microwave plasma method. However, Ravi and Joshi [16] insisted that the morphology of diamond films produced by the CVD combustion method was a strong function of temperature with temperatures below 1000 °C resulting in an octahedral habit, and with temperatures above 1000 °C resulting in a cubic habit. They did not report the gas flow ratio $R$ of oxygen to acetylene. Hanssen *et al.* [8] and Carrington *et al.* [14] showed the dependency of faceted diamond crystals on substrate temperature and $R$. They observed ball-like structures at $R$ less than 0.9 and well-faceted crystals between 0.9 and 1.08 depending on the substrate temperature. The temperature range for well-faceted crystals was 650–850 °C at $R = 0.9$ and 700–1150 °C at $R = 1.05$, showing the expansiveness of

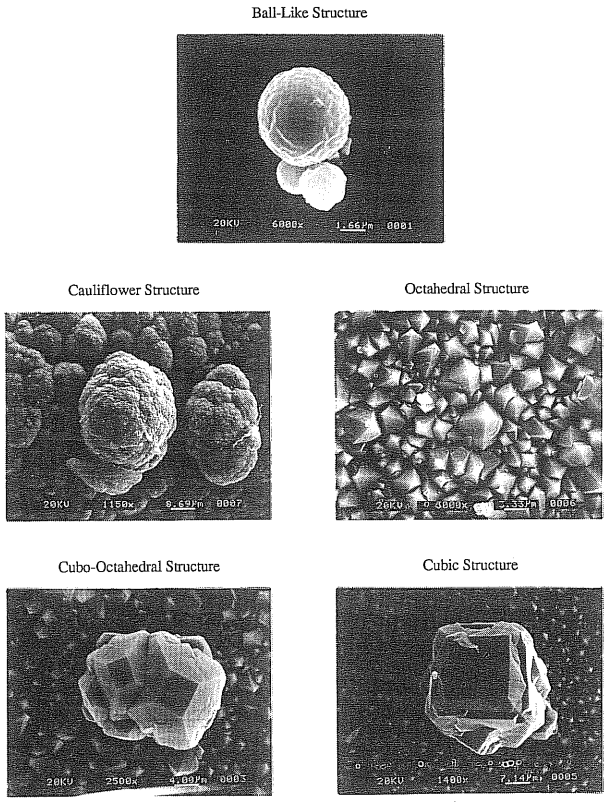


Fig. 3. Typical diamond crystal structures produced by the oxyacetylene combustion method.

the temperature range with increasing $R$ (see Fig. 4). Beyond $R = 1.1$ no diamond crystal was seen. They classified the deposit morphologies into three categories: ball like, faceted structure, and intermediate structure (like a cauliflower structure).

Recently, Nandyal [17] showed the results of his experiments regarding the effects of $R$ on diamond morphology. He made an octahedral morphology at $R = 0.94$ and $T_s = 850\ ^\circ C$ and a cubic morphology at

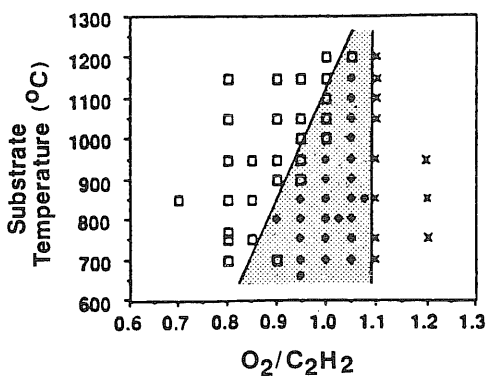


Fig. 4. Carbon growth morphology as a function of oxygen-to-acetylene ratio and substrate temperature [8]: □, ball growth; ◆, facet growth; ×, no growth; ⊡, Raman diamond peak.

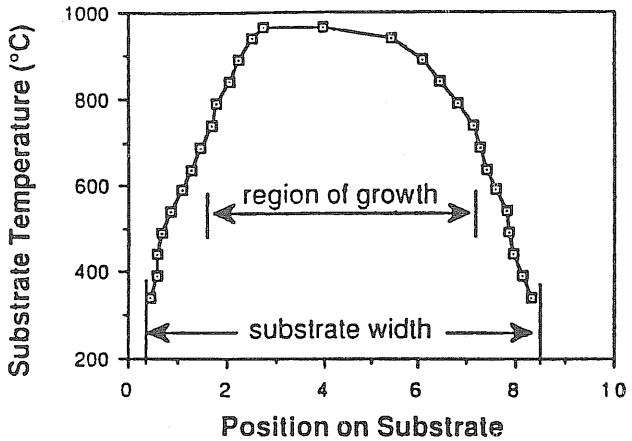


Fig. 5. Substrate temperature profile measured with a thermal imaging camera [18].

$R = 1.0$ and $T_s = 850\ ^\circ C$. One of his results is that a cubic morphology can be produced at $R \approx 1.0$.

Oakes *et al.* [18] measured the substrate surface temperature profile under typical growth conditions using a thermal imaging camera (see Fig. 5), and compared it with the observed inhomogeneities in the diamond crystallite quality. They concluded that the temperature profile on a substrate is one physical property which could contribute to this inhomogeneity.

More recently, Nandyal [17] observed that the morphology of the produced diamond film varies in the radial direction from the center of the film as shown in Fig. 6. This figure shows four distinct radial zones of a diamond film with each zone exhibiting a different morphology. However, the substrate temperature profile in the radial direction for these observations was not reported. It may be noted that prior to our recent paper [5], Fig. 5 was the only information available in the literature on the substrate surface temperature distribution.

From the results of investigations discussed here, it is evident that substrate surface temperature and gas flow ratio $R$ affect the diamond deposition on the substrate,

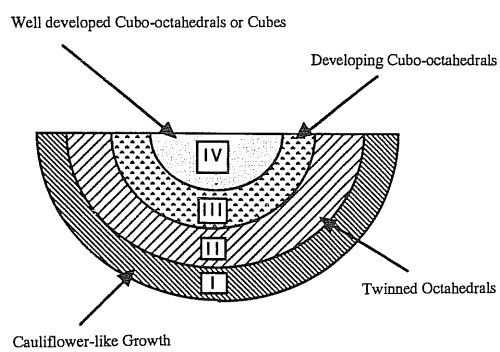


Fig. 6. Morphology distribution on a diamond film produced by the oxyacetylene combustion method [17].

and its morphology. Also, different crystal morphologies exist in the diamond films produced by the oxyacetylene combustion method, as shown in Fig. 6. However, there is no clear conclusion regarding the influence of substrate temperature and gas flow ratio, on diamond morphology. It is desirable for good quality diamond films to have uniform morphology, uniform crystal size, uniform and high crystal nucleation density, and uniform thickness. The type of particular morphology, grain size, and thickness of the diamond film depend on the application (heat transfer, tribology, manufacturing, chemical insulation, etc.). For example, cubic crystal habit is desirable for tribological applications since a diamond film with cubic crystal habit has a very smooth surface. Therefore, it is necessary to establish the relationship between temperature and $R$ on morphology, crystal nucleation density, and crystal size of the diamond film. As to the thickness of diamond film, it is more associated with total gas flow rate ($O_2 + C_2H_2$), deposition time, and nozzle size compared with the substrate temperature.

The majority of investigators using the oxyacetylene combustion method have used a non-contact temperature measurement instrument (pyrometer) to measure the substrate temperature. From the operation of a pyrometer, it is clear that the accuracy of the instrument is associated with the emittance calibration of the object whose temperature is being measured. Also, the temperature measurements by a pyrometer are influenced by the target size, area focused, changes of target emissivity with deposition of diamond film, distance between the target and the pyrometer, and the surroundings. Choi *et al.* [19] reported temperature measurement error from pyrometers during diamond deposition. They observed that temperature measurement error was induced by emittance vibration with film thickness change during the film growth process. In addition, pyrometer (because of its inherent limitations) can only detect the temperature of the target area (*i.e.* the average temperature of the area), not the temperature of a specified point. Most investigators have assumed the measured temperature to be the center temperature of the substrate surface. Furthermore, the area detected by a pyrometer varies with the working distance from the pyrometer to the target. For a typical pyrometer used in most of these experiments (Williamson 8000 series), the smallest target diameter is about 0.64 cm at a distance of 46 cm from the pyrometer. Thus, the reported temperatures are actually the average surface temperature of the detected area and not the temperature at a point and could have been influenced by a number of uncontrollable external factors. Moreover, the flame temperature varies with the radial direction as well as with the propagation direction (axial direction). Therefore, the single substrate temperatures reported by almost all of the investigators cannot be the representative substrate surface temperature as long as temperature gradients exist on the substrate surface.

As discussed earlier (see Fig. 6), the radial temperature variation of the substrate surface influences the morphology of diamond films. Therefore, it is necessary to measure accurately the radial temperature distribution of the substrate surface to study the radial morphology distribution in the diamond films produced by the oxyacetylene combustion method. This can be accomplished by using thermocouples mounted at various locations on the substrate. Use of thermocouples will reduce the influence of uncontrollable factors on the recorded temperatures.

## 3. Experimental set-up

Figure 1 above is a schematic diagram of the oxyacetylene experimental set-up used by most investigators (after ref. 13). The apparatus consists of a substrate, a water-cooled substrate holder (copper block), and an oxyacetylene welding torch fitted with a brazing nozzle. The substrate is mounted on a substrate holder to be cooled via conduction heat transfer through the copper block and convection heat transfer by continuous water (coolant) flow. To meet the objective of this study regarding the effect of substrate surface temperature on the morphology and quality of diamond films, the substrate temperature profile, the coolant flow rate and its inlet and exit temperature, the substrate position on the heat sink, and the usual parameters for the combustion synthesis method had to be carefully monitored. This required redesign of the substrate and substrate holder (heat sink). For further details see ref. 5.

Figure 7(a) shows the schematic diagram of the redesigned experimental set-up used in this investigation. The substrate is a threaded molybdenum rod. The size of the substrate is 12.7 mm in diameter and 31.75 mm in height. As discussed earlier, pyrometers do not provide an accurate and realistic temperature distribution of the substrate surface. For the accurate determination of substrate surface temperature distribution, fine-gage B-type thermocouples with the distribution shown in Fig. 7(b) and Table 1 were used. These unsheathed thermocouples have a bead diameter of approximately 0.63 mm and a wire diameter of 0.254 mm. To install these thermocouples in the substrate, the same number of small diameter holes (about 1.7 mm) were drilled on the back of the substrate to a depth of approximately 0.5 mm below the substrate surface. The thermocouples were placed in 1.6 mm diameter ceramic insulators and inserted in the back of

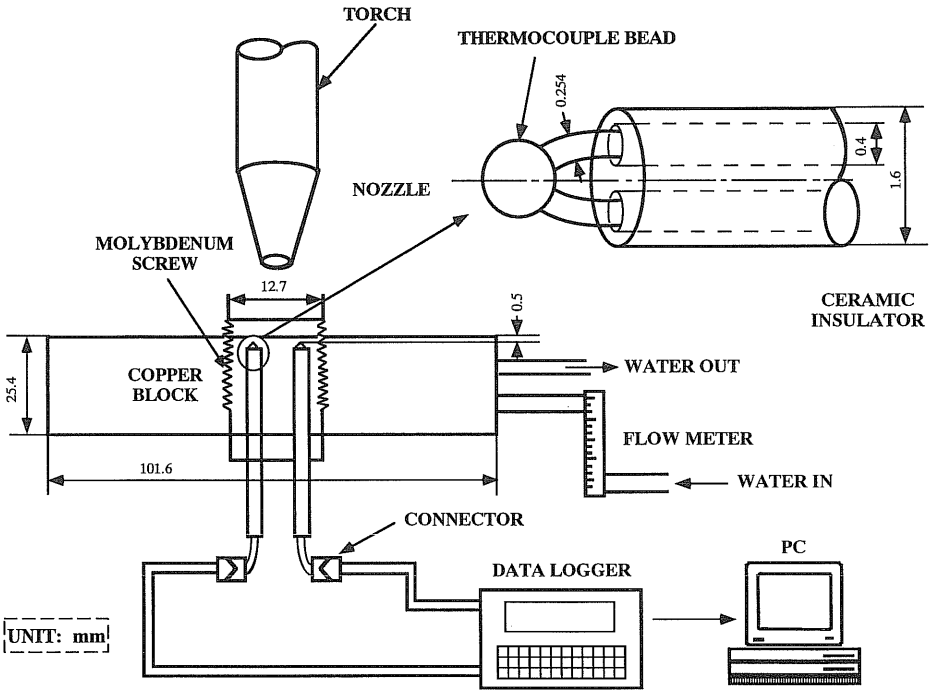


Fig. 7. (a) Schematic of the overall experimental set-up.

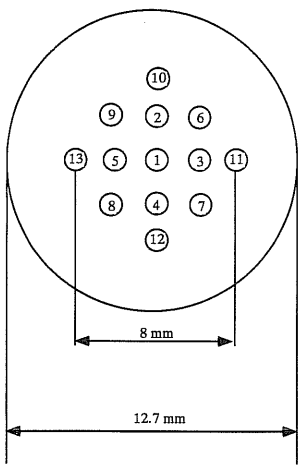


Fig. 7. (b) Distribution of thermocouples in the substrate.

TABLE 1. Distribution of thermocouple in Fig. 7(b)

| Thermocouple station | Distance from center (mm) |
|---|---|
| 1 | 0.0 |
| 2, 3, 4, 5 | 2.0 |
| 6, 7, 8, 9 | 3.0 |
| 10, 11, 12, 13 | 4.0 |

the substrate through the drilled holes. To maintain a good contact between the thermocouple beads and the substrate, a specially designed spring-loaded thermocouple holder plate was used. The thermocouples were monitored with a 40-channel Electronics Controls Design datalogger interfaced with a personal computer. Steady state temperature readings were taken at 30 s intervals. The measured temperatures were then divided by the run time to give the average temperature for each thermocouple station. Calibration of the thermocouples showed an accuracy of $\pm 1\%$ of the reading.

The molybdenum substrate described above was threaded and mounted at the center of a water-cooled copper block (see Fig. 7(a)). The copper block is 10.16 cm in diameter and 2.54 cm in height with a threaded center hole diameter of 12.7 mm (same as the substrate rod). Coolant (water) flows inside the copper block to dissipate heat from the substrate and upper surface of copper block. The coolant flow rate was monitored using a calibrated rotameter with full-scale accuracy of $\pm 2\%$ and full-scale repeatability of $\pm 1\%$. The inlet and exit temperatures were monitored with two T-type thermocouples. The accuracy of these thermocouples is $\pm 0.5$ °C.

In addition to the apparatus shown in Fig. 7(a), the experimental set-up includes two mass flow controllers (MKS type 2259C) and a mass flow programmer (MKS type 147B). The former are used to meter the gas flow rates of oxygen and acetylene, and the latter is used to program the flow rates desired and control the individual mass flow controllers with an accuracy of $\pm 0.8\%$ of full scale. Welders-grade acetylene (99.6%

purity grade) and oxygen (99.9% purity grade) were used as the reactant gases.

As the diamond crystallites in the films are of the order of micrometers in size, a scanning electron microscope was used for the morphological studies. For this purpose an ISI-ABT32 digital scanning electron microscope with a resolution of 5 nm was used. The microscope also has a built-in polaroid camera for taking micrographs of the specimens.

## 4. Results and discussion

Results of five selected experiments will be presented here. They are referred to as EXP1–EXP5. EXP1 and EXP2 used a larger nozzle ($D_n = 1.067$ mm), while the others used a smaller nozzle ($D_n = 0.939$ mm). The experiments were conducted with the centerline of the combustion flame perpendicular to the substrate surface, and constant oxygen and acetylene cylinder pressures of 20 lbf in$^{-2}$ g and 10 lbf in$^{-2}$ g respectively. The ratio of oxygen to acetylene flows rates $R$ was fixed at 0.98, but the oxygen flow rate $\dot{Q}_{O_2}$, varied from 2.5 to 3.13 standard l min$^{-1}$. The inner cone–substrate distance $L_s$, was kept at 4 mm throughout the experiments. The coolant flow rate $\dot{Q}_{H_2O}$, was varied from 0.76 to 2.46 min$^{-1}$, and the heat sink–substrate distance $H_s$ from 2 to 7 mm. The specific experimental conditions used for the five experiments are tabulated in Table 2 (for a description of the parameters listed refer to the nomenclature section of the paper). Before placing the substrate into the $O_2$–$C_2H_2$ combustion flame for the deposition of diamond film, the substrate surface was scratched with 6 μm diamond paste and cleaned by methanol. Scratching the substrate surface with diamond is found to facilitate the diamond nucleation. The scratching for each experiment was repeated the same way to ensure nearly the same initial substrate surface condition. In Figs. 8–15 below, along with the substrate surface temperature profiles a number of scanning electron micrographs of the diamond films are presented. In the micrographs, two different magnifications of 700× and 7000× were used.

To ensure reproducibility of the results, the initial conditions of the experiments were carefully controlled and each experiment was repeated two or three times. The results of these runs compared very well. It is interesting to note that during the reproducibility runs it was discovered that, when the amount of oxygen or acetylene in the cylinder was low, the combustion flame became unstable due to flow fluctuation and the results were not reproducible. Unstable flames causes a continuous change in the chemical reactions associated with growth and etching processes. However, as mentioned before, the results reported in this study were reproducible and were obtained with stable combustion flame.

### 4.1. EXP1

Figure 8 shows the morphology and substrate temperature distribution in the radial direction. It should be noted that due to the experimental limitations the substrate temperature profile was measured up to a

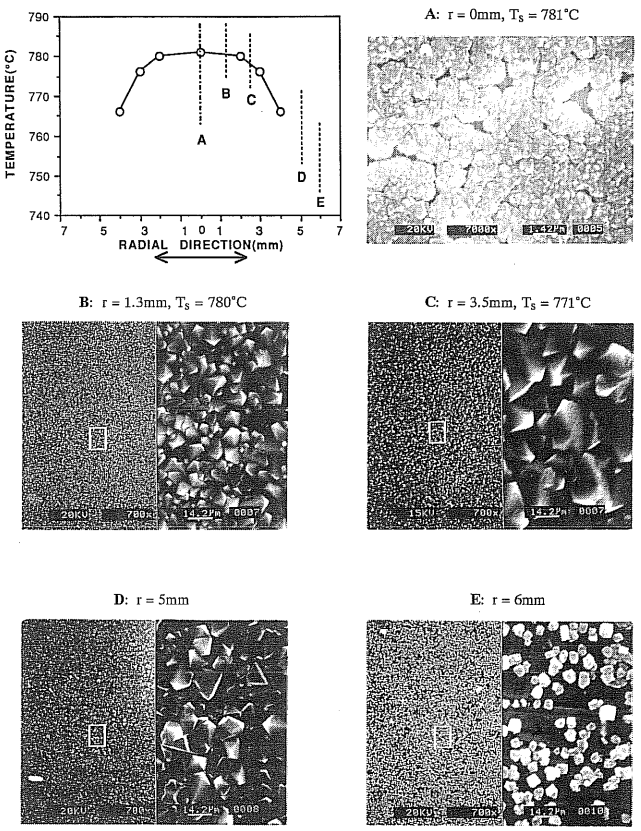


Fig. 8. Substrate temperature profile and optical observation of the film for EXP1 ($D_n = 1.067$ mm, $\dot{Q}_{O_2} = 2.5$ standard l min$^{-1}$, $H_s = 7$ mm, $\dot{Q}_{H_2O} = 0.76$ l min$^{-1}$).

TABLE 2. Experimental conditions

| | $D_n$ (mm) | $\dot{Q}_{O_2}$ (standard l min$^{-1}$) | $\dot{Q}_{C_2H_2}$ (standard l min$^{-1}$) | $H_s$ (mm) | $L_n$ (mm) | $\dot{Q}_{H_2O}$ (l min$^{-1}$) | $t_d$ (min) |
|---|---|---|---|---|---|---|---|
| EXP1 | 1.067 | 2.5 | 2.55 | 7 | 17 | 0.76 | 110 |
| EXP2 | 1.067 | 2.5 | 2.55 | 7 | 17 | 2.46 | 110 |
| EXP3 | 0.939 | 3.0 | 3.06 | 7 | 16 | 1.13 | 60 |
| EXP4 | 0.939 | 3.0 | 3.06 | 2 | 16 | 1.13 | 60 |
| EXP5 | 0.939 | 3.13 | 3.19 | 7 | 15 | 1.13 | 50 |

radius of 4 mm from the center of the substrate (see Fig. 7(b)). As shown in the figure, there is a cauliflower crystal structure at the center of the produced diamond film ($T_s \approx 781$ °C). At this region there are also some small areas where crystals have not grown. At $r = 1.3$ mm ($T_s \approx 780$ °C), an octahedral crystal structure is observed. At that radius, the length of a side of the square base $L_b$ is less than approximately 0.8 μm. The film has this type of morphology for a radius up to 5 mm, except at the center. Also, the sizes of the octahedral crystals are different in the radial direction. $L_b$ varies up to 1.4 μm at $r = 3.5$ mm ($T_s \approx 771$ °C), and varies up to 1.0 μm at $r = 5$ mm. Examining the micrographs at each radius, the grain size seen at $r = 3.5$ mm is relatively uniform compared with others.

For a radius greater than 5 mm, the micrograph in Fig. 8 shows empty areas, which means the nucleation density is very low in this region. This is more pronounced at the edge of the film ($r = 6$ mm). The diameter of this film was approximately 12 mm.

In summary, an octahedral crystal structure is the dominant morphology with larger grains at $r = 3.5$ mm and smaller grains at the center and edge. Empty areas (low nucleation density) become prominent at the edge of the film, which is common through all the experiments conducted in this study.

### 4.2. EXP2

The conditions of this experiment were identical to those for EXP1, except that the coolant flow rate was increased from 0.76 to 2.46 l min$^{-1}$. The resulting temperature levels for EXP2 are lower than those of EXP1.

From the micrographs in Fig. 9, the produced film has a ball-like crystal structure at the center ($T_s \approx 744$ °C) with very low nucleation density. A cauliflower crystal structure is seen at $r = 1$ mm ($T_s \approx 743$ °C) while the dominant morphology at $r > 1$ mm is an octahedral crystal structure. The nucleation density is low at $r > 4$ mm ($T_s \approx 718$ °C at $r = 4$ mm). The diameter of this film was 9.5 mm which is smaller than the resulting film from EXP1.

A comparison of results for EXP1 and EXP2 is shown in Fig. 10. The temperature profile for EXP2 has a higher temperature gradient at the edge due to a higher coolant flow rate. Thus, more heat dissipation occurs in the radial direction to the heat sink, resulting in lower temperatures for EXP2. These lower temperatures in the radial direction cause a smaller diameter of diamond film $D_f$ to be produced. The value of $D_f$ for EXP2 is 2.5 mm smaller than $D_f$ for EXP1. Our experiments at a fixed value of $R = 0.98$ showed that below about 680 °C diamond crystals cannot be produced. The temperature levels for EXP2 drop below the lower temperature limit at approximately $r > 4.8$ mm. Thus, the diameter of the diamond film was limited to 9.5 mm.

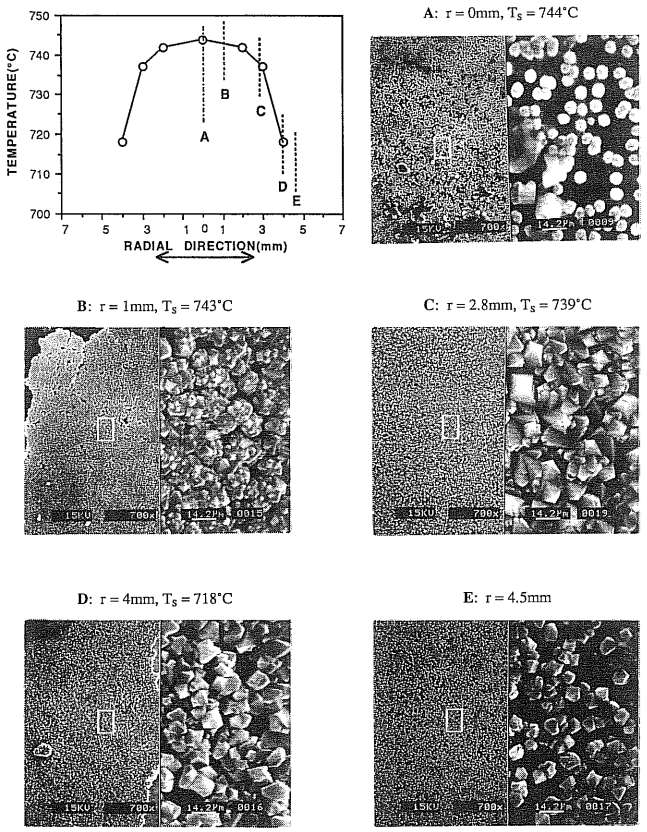


Fig. 9. Substrate temperature profile and optical observation of the film for EXP2 ($D_n = 1.067$ mm, $\dot{Q}_{O_2} = 2.5$ standard l min$^{-1}$, $H_s = 7$ mm, $\dot{Q}_{H_2O} = 2.46$ l min$^{-1}$).

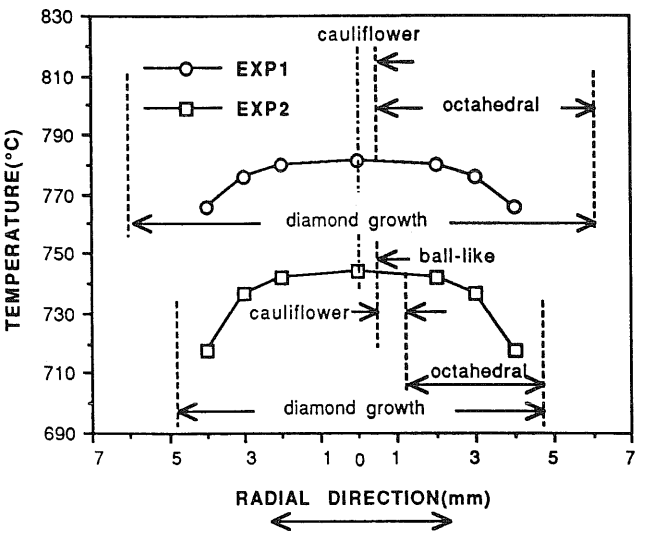


Fig. 10. Comparison of substrate temperature profiles and film morphologies for EXP1 and EXP2 ($\dot{Q}_{H_2O} = 0.76$ l min$^{-1}$ in EXP1, $\dot{Q}_{H_2O} = 2.46$ l min$^{-1}$ in EXP2).

The manner in which the morphology is distributed is also affected by the temperature profile. The dominant morphology is an octahedral crystal structure. How-

ever, a cauliflower crystal structure was found at the center for EXP1, while a ball-like crystal structure with low nucleation density was seen at the center for EXP.

### 4.3. EXP3

The results of this experiment are shown in Fig. 11. The nozzle diameter is 0.939 mm which is smaller than that used for EXP1 and EXP2. Also, the temperature levels are much higher than in EXP1 and EXP2.

Two different groups of grain sizes are present at the center ($T_s \approx 938$ °C). The group of small grains have an octahedral structure and the group of large grains consist of multifold twinned crystallites with octahedral and cubo-octahedral structures as shown in Fig. 11. The portion of small grains decreases in the radial direction from the center. Large grains are dominant at $r > 1.5$ mm ($T_s \approx 923$ °C at $r = 1.5$ mm, $T_s \approx 899$ °C at $r = 4$ mm). In this region, the large grains have the same crystallite structure as described at the center. At each radius, the nucleation density is uniform and high. The distribution of grain size is smaller at the center and the edge, but larger in the region in between. The largest grain size is seen at $r = 2$ mm. The diameter of the diamond film $D_f$, was 9.0 mm. The reason diamond film is not produced over the entire substrate diameter (12 mm) is due to the smaller nozzle diameter. A smaller $D_n$ causes a smaller acetylene feather diameter which reduces the diamond deposition area.

### 4.4. EXP 4

The conditions in this experiment are the same as in EXP3, except that the distance from the top of the substrate to the heat sink $H_s$, is decreased from 7 to 2 mm. The resulting temperature profile ($T_s \approx 722$ °C at the center, $T_s \approx 676$ °C at $r = 4$ mm) and morphology are shown in Fig. 12. The morphology is similar to what is seen in Fig. 11 for EXP3 (a single octahedral structure and multifold twinned crystallites with octahedral structure and a small presence of cubo-octahedral structure).

The largest grain size is seen at $r = 2$ mm ($T_s \approx 719$ °C). The distribution of grain size is also similar to that in EXP3, smaller at the center and edge and larger in the region in between. The diameter of the produced diamond film $D_f$, was approximately 7.5 mm.

A comparison of the results for EXP3 and EXP4 is shown in Fig. 13. Lowering the value of $H_s$ from 7 to 2 mm has an extreme effect on the temperature profile for EXP4. The difference in temperature at each radius is about 220 °C. As was the case for EXP2, as the temperature is lowered the diameter of the diamond film decreases. If the temperature drops below the lower limit of 680 °C, no film will be produced. As can be seen in Fig. 13, the temperature profile for EXP4 drops below 680 °C at the same radius where the diamond crystal is no longer seen. The morphology of EXP4 is similar to that for EXP3, except that there is more of a presence of the cubo-octahedral crystals in EXP3. The dominant morphology in EXP4 is an octahedral

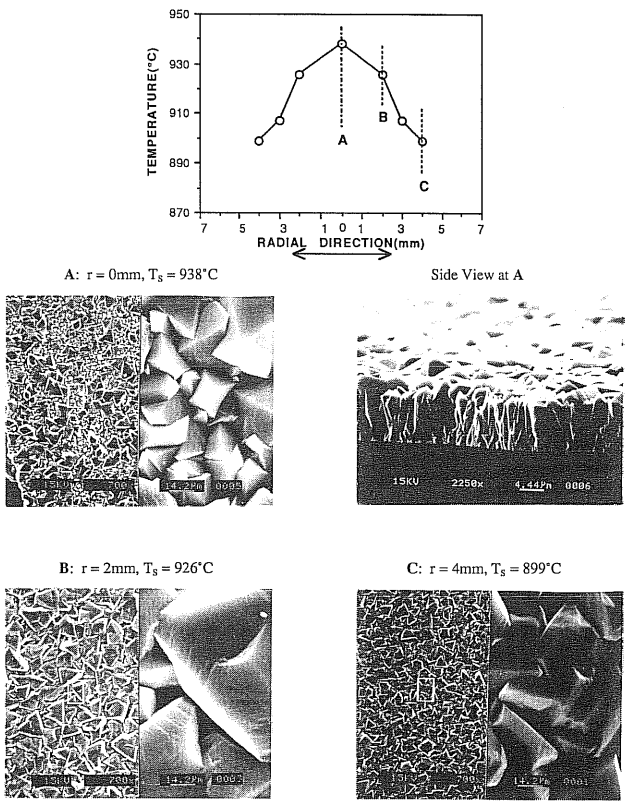


Fig. 11. Substrate temperature profile and optical observation of the film for EXP3 ($D_n = 0.939$ mm, $\dot{Q}_{O_2} = 3.0$ standard $1\,min^{-1}$, $H_s = 7$ mm, $\dot{Q}_{H_2O} = 1.13\,l\,min^{-1}$).

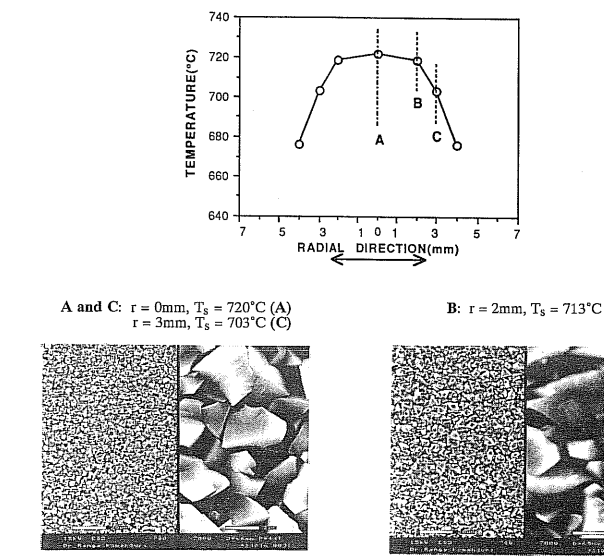


Fig. 12. Substrate temperature profile and optical observation of the film for EXP4 ($D_n = 0.939$ mm, $\dot{Q}_{O_2} = 3.0$ standard $1\,min^{-1}$, $H_s = 2$ mm, $\dot{Q}_{H_2O} = 1.13\,l\,min^{-1}$).

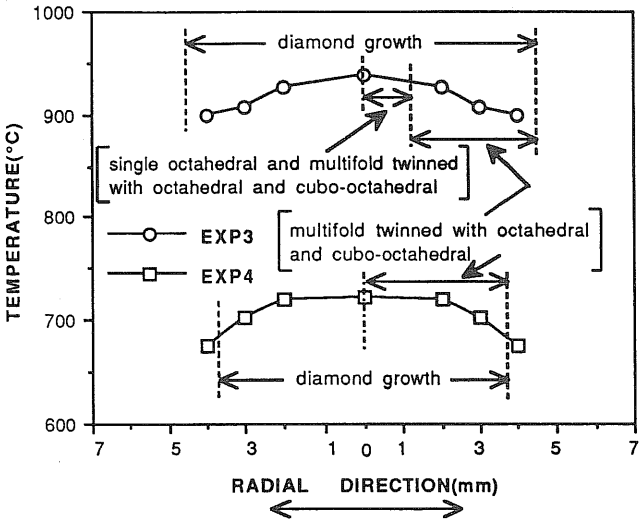


Fig. 13. Comparison of substrate temperature profiles and film morphologies for EXP3 and EXP4 ($H_s = 7$ mm in EXP3, $H_s = 2$ mm in EXP4).

structure. Also, the grain size in EXP3 is larger than the grain size in EXP4. The value of $L_b$ ranges up to 10 μm for EXP3 and up to 4 μm for EXP4.

### 4.5. EXP5

The same conditions exist for EXP5 as for EXP3, except that the gas flow rates ($\dot{Q}_{O_2}$ and $\dot{Q}_{C_2H_2}$) were increased. The gas flow ratio was kept the same as for all the experiments ($R = 0.98$). The temperature profile ($T_s \approx 1059$ °C at the center, $T_s \approx 1023$ °C at $r = 4$ mm) and morphology are shown in Fig. 14.

Well-developed cubo-octahedral structure and a multifold twinned crystallite with octahedral and cubo-octahedral structures is found at each radius, except at the center where an octahedral structure is present. The distribution of grain size is similar to that in all the previous experiments: smaller at the center and edge and larger in the region in between. The smaller grain size $L_b$ seen at the center varied up to 4 μm while the larger grain at $r = 2$ mm ($T_s \approx 1056$ °C) varied up to 9 μm. The diameter of the produced diamond film was 10 mm.

A comparison of the results for EXP3 and EXP5 is shown in Fig. 15. The temperature levels for EXP5 exceed 1000 °C and are higher than those for EXP3. The higher temperatures are due to the high gas flow rates. A cubo-octahedral structure shows up more in the morphology distribution on the resulting diamond film from EXP3 compared with the previous lower temperature experiments. Also, this structure is the dominant morphology in EXP5. This indicates that the cubo-octahedral structure begins to be produced at a higher temperature (around 900 °C) and becomes the dominant morphology at temperatures above 1000 °C.

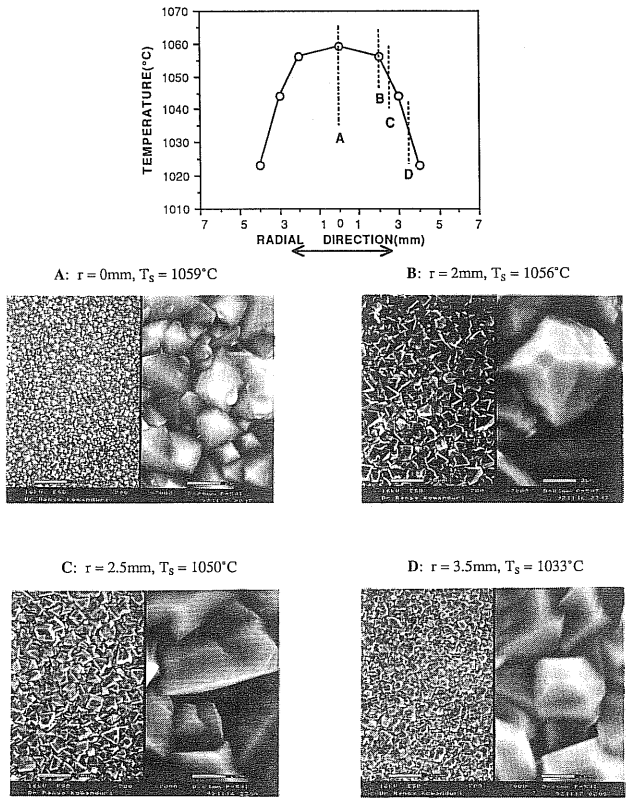


Fig. 14. Substrate temperature profile and optical observation of the film for EXP5 ($D_n = 0.939$ mm, $\dot{Q}_{O_2} = 3.13$ standard $1\,min^{-1}$, $H_s = 7$ mm, $\dot{Q}_{H_2O} = 1.13\,l\,min^{-1}$).

The diameter of the diamond film ($D_f = 10$ mm) for EXP5 was larger than that of EXP3 ($D_f = 9$ mm) due to the change in gas flow rates. An increase in the gas flow rate increases the diameter of the actylene feather. Thus more substrate area is covered by the acetylene feather causing a larger diameter of diamond film.

### 4.6. Comparison of results

A brief analysis of the diamond films produced by the five experiments and the resulting substrate surface temperatures are shown in Table 3 (for a description of the parameters listed refer to the nomenclature section of the paper). The table summarizes the results of EXP1–EXP5 shown in Figs. 8–15 with respect to the film size $D_f$, grain size $L_b$, observed morphology, and the measured substrate surface temperature. All parameters influencing substrate surface temperature profile and diamond film quality can be divided into two groups of internal and external parameters. Change of internal parameters such as $D_n$, $\dot{Q}_{O_2}$, $\dot{Q}_{C_2H_2}$, and $R$ causes change in the combustion field. As shown in Table 3, diamond grain size increases with increasing substrate surface temperature by change of the external parameters ($\dot{Q}_{H_2O}$ and $H_s$). Comparisons of $L_b$ values in EXP1 ($\dot{Q}_{H_2O} = 0.76\,l\,min^{-1}$) and EXP2 ($\dot{Q}_{H_2O} = 2.46\,l\,min^{-1}$), and $L_b$ values EXP3 ($H_s = 7$ mm) and

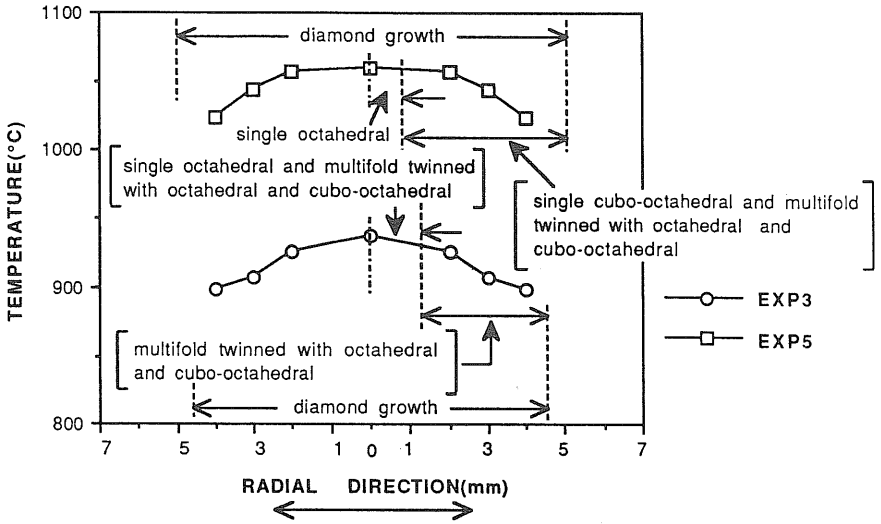


Fig. 15. Comparison of substrate temperature profiles and film morphologies for EXP3 and EXP5 ($\dot{Q}_{O_2} = 3.0$ standard $l\,min^{-1}$ in EXP3, $\dot{Q}_{O_2} = 3.13$ standard $l\,min^{-1}$ in EXP5).

TABLE 3. Summary of experimental results

| | $D_f$ (mm) | $L_b$ (mm) | Morphology | Substrate temperature (°C) | |
|---|---|---|---|---|---|
| | | | | $r = 0$ | $r = 4$ mm |
| EXP1 | 12 | ~ 1.4 | Cauliflower, octahedral | 781 | 766 |
| EXP2 | 9.5 | ~ 1.2 | Ball like, cauliflower, octahedral | 744 | 718 |
| EXP3 | 9.0 | ~10.0 | Octahedral, cubo-octahedral | 938 | 899 |
| EXP4 | 7.5 | ~ 4.0 | Octahedral | 722 | 676 |
| EXP5 | 10.0 | ~ 9.0 | Octahedral, cubo-octahedral | 1059 | 1023 |

EXP4 ($H_s = 2$ mm), support this relation of grain size to substrate surface temperature. Also, diamond grain size increases with decreasing $D_n$ ($D_n = 1.067$ mm in EXP1 and EXP2, $D_n = 0.939$ mm in EXP3, EXP4 and EXP5) as shown in Table 3. In the case of small nozzle size, well-developed crystals (octahedral and cubo-octahedral structures) are produced through the entire film. Prediction of grain size and morphology is very important for proper application of diamond films.

The resulting film diameters are different depending on the experimental conditions as shown in Table 3. $D_f$ is related to the flame shape and substrate surface temperature. As discussed earlier, the acetylene feather should be wide with $T_s > 680$ °C for a large $D_f$. The width of the acetylene feather increases with increasing internal parameters ($D_n$ and $\dot{Q}_{O_2}$) at the same value of $R$. Thus $D_f$ increases with increasing $D_n$ and $\dot{Q}_{O_2}$. Comparisons of $D_f$ values of EXP1 and EXP2 ($D_n = 1.067$ mm) with those of EXP3, EXP4 and EXP5 ($D_n = 0.939$ mm), and $D_f$ of EXP3 ($\dot{Q}_{O_2} = 3.0$ standard $l\,min^{-1}$) with that of EXP5 ($\dot{Q}_{O_2} = 3.13$ standard $l\,min^{-1}$), support this relation of $D_f$ to $D_n$ and $\dot{Q}_{O_2}$ with the same value of $R$. The understanding of the resulting $D_f$ values from different experimental conditions is essential to the development of a combustion CVD method for large-area coating by using a moving single-nozzle system or a multinozzle system.

The diamond growth rates for the five experiments presented in this study ranged from 10 to 20 $\mu m\,h^{-1}$. The Reynolds number based on the nozzle diameter ($Re = \rho V D_n/\mu$, where $\rho$ and $\mu$ are the density and absolute viscosity of the mixed gas at room temperature, $V$ is the gas velocity at the exit of the nozzle, and $D_n$ is the nozzle diameter) for the five experiments ranged from about 7900 to 11 200, which makes the combustion flame turbulent [20, 21]. According to Snail and Craigie [20] and Snail *et al.* [21], diamond films grown in a turbulent flame have growth rates lower than those in a laminar flame. However, the quality of diamond films produced in a turbulent flame is better than those in a laminar flame. Their reported [20, 21] diamond growth rates in a turbulent combustion flame were from 10 to 30 $\mu m\,h^{-1}$ which is in agreement with the growth rates observed in this study.

The specific results presented in this study for a molybdenum substrate are fairly dependent on the sub-

strate material. Different substrate materials commonly used in oxyacetylene combustion CVD diamond synthesis, such as silicon or tungsten, will produce different specific results due to the differences in the thermophysical properties of the materials. That is, different substrate surface temperature distribution and substrate material would lead to different grain size and morphology distributions for the produced diamond films. However, the general behavior of the results of this study should be applicable to other substrates. The effect of substrate material on the morphology and quality of diamond films should be further investigated.

## 5. Conclusions

In this paper, it was established that the morphology and quality of a diamond film have a strong relation to the substrate temperature profile and nozzle size. The substrate surface temperature profiles were changed by varying several process parameters such as the coolant flow rate, the substrate–heat sink distance, the oxygen and acetylene flow rates, and the nozzle size. The lower temperature limit for diamond deposition (nucleation) with $R = 0.98$ is about 680 °C. The size of the diamond crystal (grain) has a tendency of increasing with increasing temperature. Experiments with small nozzle size provides good quality diamond films since the produced film had relatively uniform morphology. For proper application of synthetic diamond films produced by the oxyacetylene combustion mothod, the effects of substrate surface temperature and nozzle size on the morphology and quality of these films should be considered.

## Acknowledgments

Support for this research was partially provided by the Oklahoma State University center for Energy Research (Grant 1150748) and the Oklahoma Center for Integrated Design and Manufacturing.

## Nomenclature

| | |
|---|---|
| $D_f$ | diameter of the synthetic diamond film |
| $D_n$ | nozzle diameter (see Fig. 1) |
| $H_s$ | substrate height (see Fig. 1) |
| $L_b$ | length of a side of the square base in octahedral or cubo-octahedral crystals |
| $L_i$ | length of the inner cone (see Fig. 1) |
| $L_n$ | distance between the substrate surface and tip of the nozzle (see Fig. 1) $L_s + L_i$ |
| $L_s$ | distance from the substrate surface to the inner cone (see Fig. 1) |
| $\dot{Q}_{C_2H_2}$ | volume flow rate of acetylene |
| $\dot{Q}_{H_2O}$ | volume flow rate of water |
| $\dot{Q}_{O_2}$ | volume flow rate of oxygen |
| $R$ | ratio of volume flow rates of oxygen to acetylene |
| $t_d$ | deposition time |
| $T_s$ | substrate temperature |

## References

1 R. C. DeVries, Synthesis of diamond under metastable conditions, *Annu. Rev. Mater. Sci.*, *17* (1987) 161.
2 J. C. Angus and C. C. Hayman, Low-pressure, metastable growth of diamond and diamond like phases, *Science*, *241* (1988) 913–921.
3 B. Lux and R. Haubner, Low pressure synthesis of superhard coatings, *Int. J. Ref. Hard Met.*, (1989) 158–174.
4 A. G. Gaydon and H. G. Wolfhurd, *Flames: Their Structures, Radiation, and Temperature*, 4th edn., Chapman and Hall, New York, 1979.
5 A. J. Ghajar and K. Bang, Parametric effects on the substrate temperature profile in oxy-acetylene flames, *Heat Transfer Eng.*, *14* (1993) 48–59.
6 P. G. Kosky and D. S. McAtee, An experimental and theoretical investigation of flame-formed diamond, *Mater. Lett.*, *8* (1989) 369–374.
7 W. A. Yarbrough, M. A. Stewart and J. A. Cooper, Jr., Combustion synthesis of diamond, *Surf. Coat. Technol.*, *39–40* (1989) 241–252.
8 L. M. Hanssen, K. A. Snail, W. A. Carrington, J. E. Butler, S. Kellogg and D. B. Oakes, Diamond and non-diamond carbon synthesis in an oxygen–acetylene flame, *Thin Solid Films*, *196* (1991) 271–281.
9 R. Komanduri, K. S. Snail and L. L. Fehrenbacher, Growth of diamond crystals by combustion synthesis, *Philos. Mag. Lett.*, *62* (1990) 283–290.
10 M. A. Cappelli and P. H. Paul, An investigation of diamond film deposition in a premixed oxyacetylene flame, *J. Appl. Phys.*, *67* (1990) 2596–2603.
11 Y. Tzeng, C. Cutshaw, R. Phillips and T. Srivinyunon, Growth of diamond films on silicon from an oxygen–acetylene flame, *Appl. Phys. Lett.*, *56* (1990) 134–136.
12 Y. Hirose, S. Amanuma and K. Kunio, The synthesis of high-quality diamond in combustion flames, *J. Appl. Phys.*, *68* (1990) 6401–6405.
13 L. M. Hanssen, W. A. Carrington, J. E. Butler and K. A. Snail, Diamond synthesis using an oxygen–acetylene torch, *Mater. Lett.*, *7* (1988) 289.
14 W. A. Carrington, L. M. Hanssen, K. A. Snail, D. B. Oakes and J. E. Butler, Diamond growth in $O_2 + C_2H_4$ and $O_2 + C_2H_2$ flames, *Metall. Trans. A*, *20* (1989) 1282–1284.
15 S. Matsumoto and Y. Matsui, Electron microscopic observation of diamond particles growth from the vapor phase, *J. Mater. Sci.*, *18* (1983) 1785–1793.
16 K. V. Ravi and A. Joshi, Evidence for ledge growth and lateral epitaxy of diamond single crystals synthesized by the combustion flame technique, *Appl. Phys. Lett.*, *58* (1991) 246–248.
17 S. Nandyal, Combustion synthesis of diamond films, *M. S. thesis*, Oklahoma State University, Stillwater, OK, 1991.
18 D. B. Oakes, J. E. Butler, K. A. Snail, W. A. Carrington and L. M. Hanssen, Diamond synthesis in oxygen–acetylene flames: inhomogeneities and the effect of hydrogen addition, *J. Appl. Phys.*, *69* (1991) 2602–2610.

19 B. I. Choi, M. I. Flik and A. C. Anderson, Adaptively calibrated pyrometry for film deposition processes, in J. C. Khanpara and P. Bishop (eds.), *Heat Transfer in Materials Processing*, Vol. 224, American Society of Mechanical Engineers, New York, 1992, pp. 19–26.

20 K. A. Snail and C. J. Craigie, Synthesis of high quality diamond films in a turbulent flame, *Appl. Phys. Lett.*, *58* (1991) 1875–1877.

21 K. A. Snail, C. L. Vold, C. M. Marks and J. A. Freitas, Jr., High-temperature epitaxy of diamond in a turbulent flame, *Diamond Relat. Mater. 1* (1992) 180–186.